

·临床研究·

多参数磁共振成像联合表观弥散系数直方图分析预测膀胱癌的病理分化

孔令敏¹, 凌 坚², 蔡 迁¹, 温志华¹, 郭 燕¹, 王焕军¹

(1. 中山大学附属第一医院放射科, 广东广州 510080; 2. 中山大学附属第一医院东院放射科, 广东广州 510700)

摘 要:【目的】探讨多参数磁共振成像联合表观弥散系数(ADC)直方图分析应用于膀胱癌合并其他病理分化类型的预测价值。【方法】回顾性收集并分析2015年3月至2023年3月就诊于中山大学附属第一医院并经手术病理证实为膀胱尿路上皮癌患者的临床及影像学资料。根据术后病理结果,将患者分为有合并其他病理分化(如鳞状分化、腺样分化等)组及无其他病理分化组。运用倾向性评分匹配的方法,将无分化组患者按年龄及性别与有分化组患者进行两组间1:1最邻近匹配,两组均入组49例。使用ITK-SNAP软件在ADC对患者病灶全层勾画并将其导入开源软件Pyradiomics提取直方图特征。比较两组间膀胱癌患者的临床、病理及影像参数差异,计算受试者工作特征曲线(ROC)的曲线下面积(AUC)评估各参数鉴别膀胱癌有无分化的诊断效能。采用多因素logistic回归筛选独立危险因素,以此构建临床模型。【结果】病灶形态、VI-RADS评分、强化特点及周围是否有可疑淋巴结肿大在两组间差异有统计学意义($P < 0.05$)。有分化组ADC均数、第10、25、75和90百分位数均小于未分化组($P < 0.05$)。多因素logistic回归分析发现,病灶强化特点、ADC平均数及第25、75百分位数为独立预测因子($P < 0.05$),构建联合模型,其诊断效能最优[AUC (95%CI) = 0.91 (0.83, 0.96)]。【结论】多参数磁共振成像联合ADC直方图分析可准确预测膀胱癌患者是否合并其他病理分化,可协助临床制定更个体化的治疗方案。

关键词:膀胱肿瘤;尿路上皮;磁共振成像;直方图;分化

中图分类号:R445.2

文献标志码:A

文章编号:1672-3554(2023)06-1008-08

DOI:10.13471/j.cnki.j.sun.yat-sen.univ(med.sci).2023.0615

Multiparametric MRI Combined with Apparent Diffusion Coefficient Histogram Analysis for Assessing Variant Histology in Urothelial Carcinoma

KONG Ling-min¹, LING Jian², CAI Qian¹, WEN Zhi-hua¹, GUO Yan¹, WANG Huan-jun¹

(1. Department of Radiology, The First Affiliated Hospital, Sun Yat-sen University, Guangzhou 510080, China; 2. Department of Radiology, The East Division of the First Affiliated Hospital, Sun Yat-sen University, Guangzhou 510700, China)

Correspondence to: WANG Huan-jun; E-mail: wanghj45@mail.sysu.edu.cn

Abstract:【Objective】To investigate the feasibility of multiparametric MRI (mpMRI) combined with histogram analysis of apparent diffusion coefficient (ADC) in the assessment of patients with variant histology (VH) of urothelial carcinoma (UC).【Method】We retrospectively analyzed the data of patients pathologically diagnosed with UC who underwent mpMRI in the First Affiliated Hospital of Sun Yat-sen University between March 2015 and March 2023. The patients were divided into VH group (urothelial carcinoma mixed with other histologies) and non-VH group (pure urothelial carcinoma) according to pathological results. We performed propensity score 1:1 nearest-neighbor matching on the two groups based

收稿日期:2023-06-06

基金项目:国家自然科学基金(82071989,82371911,82372075)

作者简介:孔令敏,第一作者,研究方向:医学影像学,E-mail:konglm@mail2.sysu.edu.cn;王焕军,通信作者,副主任医师,研究方向:医学影像学,E-mail:wanghj45@mail.sysu.edu.cn

on age and gender and 49 patients were included in each group. The regions of interest (ROIs) of the whole tumor were delineated manually by using ITK-SNAP software and Pyradiomics was applied to extract ADC histogram parameters. We compared the clinicopathological data, MRI morphological features and ADC histogram parameters between the groups. Multivariate logistic regression was used to identify independent risk factors and construct the prediction model. Receiver operating characteristic (ROC) curve analyses were performed to evaluate the diagnostic performance of these parameters for determining VH of UC.【Results】MRI morphological features including the lesion shape, vesical imaging-reporting and data system (VI-RADS) score, enhancement pattern and suspicious lymph node metastasis were markedly different between the two groups (all $P < 0.05$). ADC_{mean} , ADC_{median} , ADC_{25th} , ADC_{75th} , ADC_{10th} and ADC_{90th} were significantly lower in patients with VH than those in non-VH group (all $P < 0.05$). Multivariate logistic regression analysis showed enhancement pattern, ADC_{25th} , ADC_{75th} and ADC mean were independent predictors ($P < 0.05$). The combined model yielded the best predictive performance, with an area under the ROC curve (AUC) of 0.91 (95% CI: 0.83-0.96).【Conclusions】MpMRI combined with whole-tumor histogram analysis of ADC can serve as a reliable method for evaluating the presence of VH in UC, further to assist the clinical decision making.

Key words: urothelial carcinoma, urothelium, magnetic resonance imaging (MRI), histogram, quantitative; variant

[J SUN Yat-sen Univ (Med Sci), 2023, 44(6): 1008-1015]

膀胱尿路上皮癌(以下简称膀胱癌)是泌尿系统最多发的恶性肿瘤。据报道约33%的尿路上皮肿瘤可出现其他病理类型的分化^[1]。多项临床研究发现伴有其他分化亚型出现的尿路上皮肿瘤侵袭性高,易转移、复发,预后差^[2-3]。同时,该部分患者新辅助化疗、免疫治疗效果较差,易产生耐药性^[4-5]。因此,早期、准确诊断膀胱尿路上皮肿瘤是否伴有其他病理分化对患者预后判断及后续治疗方案的制定具有重要的临床意义。组织病理活检是确诊膀胱肿瘤组织出现分化的金标准。但该操作有创,且局灶性活检结果不能反映整体,常出现假阴性。现阶段膀胱癌伴有其他病理亚型出现的漏诊率可达44%~61%^[6-7],亟需其他检查方式辅助临床提高诊断准确率。多参数磁共振成像(magnetic resonance imaging, MRI)具有软组织分辨率高、无创、可重复性好等优点,已广泛用于膀胱癌的术前诊断、分期、分级以及术后复发监测^[8-10]。弥散加权成像(diffusion weighted imaging, DWI)及表观弥散系数(apparent diffusion coefficient, ADC)值可以定量评估肿瘤组织内水分子弥散运动情况,进而反映肿瘤恶性程度,是膀胱癌诊断的重要检查方式^[11]。基于全瘤体积的直方图分析方法可分析整合肿瘤内所有体素值,定量评估肿瘤组织内部异质性,被广泛应用于多个部位肿瘤的诊断和病理分级预测^[12-15]。相较于影像组学,其操作简单,便于临床医生理解,为临床治疗方案制定及预后评估提供更加可靠的参考信息。因此,本研究旨在探讨多参

数MRI联合ADC直方图分析在预测膀胱癌分化中的应用价值。

1 材料与方法

1.1 病例收集

回顾性收集2015年3月至2023年3月中山大学附属第一医院经病理证实为膀胱尿路上皮癌的患者。纳入标准:①患者术前2周内接受了MRI检查;②经手术病理证实为膀胱尿路上皮癌并判断有无合并其他病理分化。排除标准:①MRI检查前进行化疗、放疗等其他治疗;②MR图像存在严重运动伪影,影响分析。该项研究得到中山大学附属第一医院伦理委员批准(伦审[2020]492号),免除患者知情同意。

1.2 多参数磁共振图像采集

采用德国西门子Magnetom Trio以及美国GE SIGNA Pioneer 3.0T MRI系统,8和32通道相控阵线圈进行图像采集。参数如下:①横断面T1WI:TR 758 ms,TE 12 ms,FOV 220 mm,矩阵352×320,层厚4 mm,平均激励次数2次;②横断面T2WI:TR 4817 ms,TE 125.7 ms,FOV 220 mm,矩阵352×320,层厚4 mm,平均激励次数3次;③横断面DWI(b值取0,1 000 s/mm²):TR 3 904 ms,FOV 220 mm,矩阵128×128,层厚4 mm,平均激励次数1次。横断面DCE-MRI采用3D T1WI脂肪抑制梯度回波序列,平扫1期后,采用高压注射器经手背静脉注入对比

剂马根维显(拜耳药业)或钆特酸葡胺(江苏恒瑞医药股份有限公司),速率 2 mL/s,剂量 0.1 mmol/kg,之后立即团注 25 mL 生理盐水,静脉注射对比剂 14 s 后开始采集连续 5 期的动态增强扫描,单期扫描时间为 26 s。

1.3 多参数磁共振图像处理及分析指标

2 名分别具有 2 年和 6 年盆腔 MRI 诊断经验的放射科诊断医师利用 ITK-SNAP 软件(<http://www.itksnap.org/pmwiki/pmwiki.php>)分别勾勒肿瘤全层的感兴趣区域(region of interest, ROI),注意应排除肿瘤蒂、血管及相应坏死区域。然后将获得的 ROI 复制到表观弥散系数(apparent diffusion coefficient, ADC)图,获得相应 ADC 值。将图像及勾勒 ROI 导

入开源软件 Pyradiomics (www.radiomics.io/pyradiomics.html)提取全瘤体积的直方图特征,包括均值(ADC_{mean}),中位数(ADC_{median}),第 10、25、75 和 90 百分位数(ADC_{10th} , ADC_{25th} , ADC_{75th} , ADC_{90th})。

此外,上述 2 名放射科诊断医师记录膀胱内病灶影像学征象,包括①病灶形态(图 1),②病灶数目,③病灶位置,④病灶大小,⑤是否均匀强化(图 2),⑥VI-RADS 评分,⑦病灶周围有无可疑淋巴结转移(淋巴结形状、强化方式等),⑧输尿管是否扩张积液。1 名具有 13 年盆腔 MRI 诊断经验的放射科诊断医师核对上述信息准确性。出现分歧时,以讨论后结果为准。

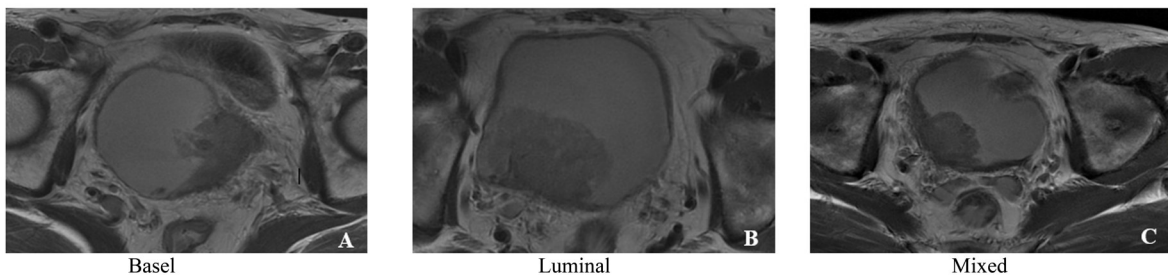


图 1 膀胱癌病灶不同的 MR 表现形态示意图

Fig. 1 Schematic diagram of the MRI morphology of urothelial carcinoma

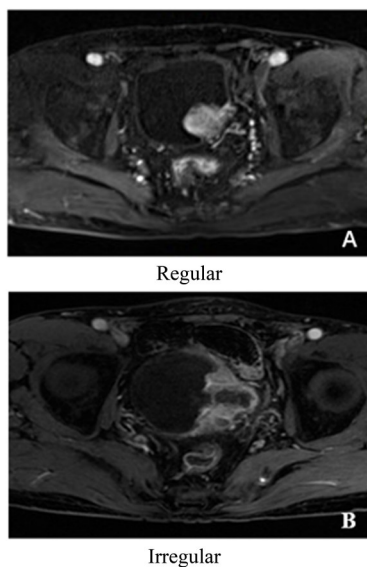


图 2 膀胱癌病灶在 MR 图像上的不同强化特点示意图

Fig. 2 Schematic diagram of the MRI enhancement pattern of urothelial carcinoma

1.4 临床及病理指标收集

在电子病历系统收集膀胱癌患者以下特征:性别、年龄、血尿症状、吸烟史及有无复发。病理科医

生根据 2016 版 WHO 泌尿男生殖系统肿瘤分类评估肿瘤病灶的组织学分级并记录其是否伴有其他组织病理分化出现。根据病理结果,将患者分为有分化组及无分化组。

1.5 统计学方法

统计学分析和统计作图采用 SPSS 25.0、R 软件 4.0.5 和 MedCalc 20.0。运用倾向性评分匹配的方法,将无分化组患者按年龄及性别与分化组患者进行 1:1 最邻近匹配,以减少两组基线变量上的差异。连续变量的正态性检验和方差齐性检验采用 Kolmogorov-Smirnov 和 Levene 检验评估,符合正态分布的定量资料用平均数 \pm 标准差表示,不符合正态分布则用中位数和四分位数 $M(P_{25} \sim P_{75})$ 表示。两组间比较采用独立样本 t 检验或 Mann-Whitney U 检验。定性资料采用例数(率)表示,使用 χ^2 检验或 Fisher 确切概率法进行组间比较。多参数 logistic 回归用于筛选出独立预测因子,排除混杂偏倚。绘制受试者工作特征曲线(receiver operating characteristic, ROC)并计算曲线下面积(area under the curve, AUC)评价各参数鉴别尿路上皮肿瘤是否伴

有病理亚型改变的诊断效能。采用DeLong检验比较不同参数AUC差异。组内相关系数(intraclass correlation coefficient, ICC)用来评估2名医师所勾画ROI获得影像学参数的一致性。ICC > 0.80视为一致性良好。所有检验采用双侧检验, $P < 0.05$ 为差异有统计学意义。

2 结果

2.1 有分化组及无分化组临床、病理及影像学征象比较

根据术后病理结果,将患者分为有分化组($n=49$)及无分化组($n=1\ 020$)。运用倾向性评分方法,根据年龄及性别1:1进行两组间最邻近匹配,最终两组均入组49例患者。两组基线资料(性别、年

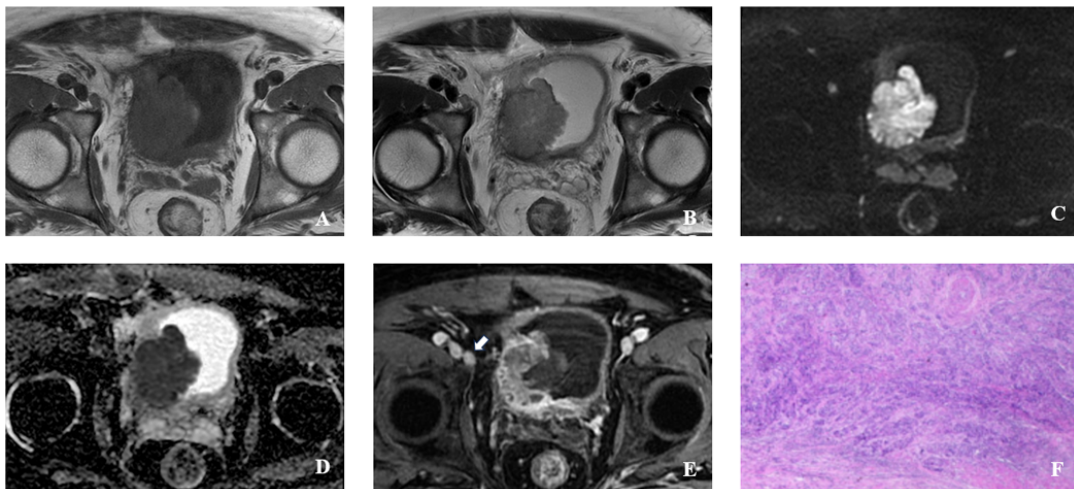
龄)相比差异无统计学意义($P > 0.05$)。有分化组病理亚型具体分类为:鳞状分化30例(61.23%),腺样分化10例(20.41%),鳞状分化同时伴有腺样分化4例(8.16%),微乳头型2例(4.08%),肉瘤亚型2例(4.08%),浆细胞亚型1例(2.04%)。两组间临床及病理指标差异均无统计学意义($P > 0.05$)。患者具体临床及病理特征见附表。



附表

Appendix table

在影像学征象方面,有分化组及未分化组间病灶形态、VI-RADS评分及其强化特点、周围有无可疑肿大淋巴结的差异均有统计学意义($P < 0.05$) (表1)。图3所示为膀胱癌伴鳞状分化患者的影像学及病理图像。



Axial T1-weighted image (A) and T2-weighted image show a tumor (6 cm) at the right lateral wall (B), medium-signal-intensity, DWI ($b=1\ 000\ \text{s}/\text{mm}^2$) shows high-signal-intensity (C) and ADC map shows low-signal-intensity (D), DCE MRI shows significantly irregular enhancement (E), there is lymph node metastasis in pelvic (arrow), verified by pathology. Finally, the tumor should be classified as VI-RADS 5 (E); microscopic image of hematoxylin-eosin staining (original magnification, $\times 100$) (F).

图3 68岁男性膀胱癌伴鳞状分化患者MR图像

Fig. 3 MRI scans in a 68-year-old man with urothelial carcinoma and a differentiation of squamous

2.2 有分化组及未分化组直方图参数比较

2名放射科医师测量的各项直方图参数有良好的-一致性(ICC:0.880~0.991)。有分化组及无分化组间 ADC_{mean} 、 $\text{ADC}_{\text{median}}$ 、 $\text{ADC}_{10\text{th}}$ 、 $\text{ADC}_{25\text{th}}$ 、 $\text{ADC}_{75\text{th}}$ 及 $\text{ADC}_{90\text{th}}$ 差异均有统计学意义($P < 0.05$;表1)。

2.3 影像学征象及表观弥散系数图直方图参数联合模型建立

在MRI征象方面,强化特点对膀胱癌伴有分化

鉴别的诊断效能最佳[AUC (95% CI) = 0.72(0.63, 0.81);表2、图4]。在ADC直方图参数中, $\text{ADC}_{90\text{th}}$ 诊断效能最佳[AUC (95% CI)=0.80 (0.71, 0.88);表3、图4]。将影像学征象及ADC直方图参数纳入多因素logistic回归分析,病灶强化特点、 ADC_{mean} 、 $\text{ADC}_{25\text{th}}$ 及 $\text{ADC}_{75\text{th}}$ 为独立预测因子($P < 0.05$;表4),构建联合模型[AUC (95% CI)=0.91 (0.83, 0.96),灵敏度=93.88%,特异度=83.67%,准确度=88.78%, $P < 0.001$;图5]。

表1 有分化组和无分化组ADC直方图参数比较
Table 1 Comparisons of ADC histogram features in VH and non-VH group

Features	Z	P	ICC
Mean(10^{-3} mm ² /s)	-3.428	0.001	0.997
Median(10^{-3} mm ² /s)	-2.640	0.003	0.994
10 th percentile(10^{-3} mm ² /s)	-2.220	0.013	0.971
25 th percentile(10^{-3} mm ² /s)	-2.203	0.013	0.989
75 th percentile(10^{-3} mm ² /s)	-3.450	0.001	0.991
90 th percentile(10^{-6} mm ² /s)	-4.508	<0.001	0.960

ADC: apparent diffusion coefficient; ICC: intraclass correlation coefficient; VH: variant histology.

3 讨论

准确判断尿路上皮癌是否伴有分化对患者风险分层、治疗方案制定及预后预测至关重要。2016年,WHO泌尿男生殖系统肿瘤分类将膀胱癌病理

亚型分为12类,包括鳞状分化、腺样分化、微乳头型、肉瘤型等^[1]。随着分子生物学发展,2022年WHO泌尿男生殖系统肿瘤分类将巢状尿路上皮癌及大巢状尿路上皮癌划分为两类,并新提出管状型分化,进一步完善病理亚型分类^[16]。与单纯尿路上皮癌相比,伴有其他病理亚型分化的膀胱癌恶性程度更高,更易复发转移^[17]。针对这部分患者,多项研究推荐应尽早行根治性膀胱切除术辅以术后化疗,以延长患者生存期,改善预后^[18-20]。现阶段临床诊断膀胱癌分化主要依靠病理组织活检,但其不仅有创,还具有取材的片面性,不能反映全瘤情况,因此常出现假阴性。因此本研究旨在探讨多参数MRI及ADC直方图参数分析与膀胱癌是否伴有病理亚型之间的关系,以期鉴别尿路上皮癌是否伴有分化提供一种新的辅助诊断方法。

本研究结果显示病灶形态、VI-RADS评分、病灶强化特点及周围是否伴有可疑淋巴结转移与膀胱癌患者是否出现分化有关($P < 0.05$)。其原因在于伴有分化的膀胱癌患者就诊时病灶常处于高分

表2 MRI征象区分有分化组和无分化组的诊断效能

Table 3 Diagnostic performance of imaging features in differentiating VH group from non-VH group

Features	AUC (95%CI)	Cutoff	Sensitivity	Specificity	Accuracy
Morphology	0.67 (0.56, 0.78)	1	48.98	83.67	66.32
Enhancement pattern	0.72 (0.63, 0.81)	1	57.14	87.76	72.45
Lymph node metastasis	0.64 (0.54, 0.74)	0	46.94	81.63	64.29
VI-RADS	0.67 (0.81, 0.95)	2	55.10	79.59	67.35

AUC: area under the curve; CI: confidence interval; VH: variant histology.

表3 ADC直方图参数区分有分化组和无分化组的诊断效能

Table 3 Diagnostic performance of ADC histogram analysis parameters in differentiating VH group from non-VH group

Features	AUC (95%CI)	Cutoff	Sensitivity	Specificity	Accuracy
Mean	0.73 (0.63, 0.81)	1.04	81.63	59.18	71.42
Median	0.68 (0.57, 0.77)	0.98	71.43	61.22	66.33
10 th percentile	0.64 (0.54, 0.74)	0.84	73.47	53.06	63.27
25 th percentile	0.65 (0.54, 0.74)	0.89	67.35	59.18	63.27
75 th percentile	0.73 (0.63, 0.81)	1.12	79.59	61.22	69.39
90 th percentile	0.80 (0.71, 0.88)	1.20	73.47	79.59	76.53

ADC: apparent diffusion coefficient; AUC: area under the curve; CI: confidence interval; VH: variant histology.

表4 预测膀胱癌分化的多因素 logistic 回归分析
Table 4 Multivariate logistic analysis for predicting

VH			
Variable	<i>P</i>	OR	OR 95% CI
Constant	0.145		
Morphology	0.851	1.104	(0.394, 3.098)
Enhancement pattern	0.016	5.815	(1.383, 24.447)
Lymph node metastasis	0.248	2.283	(0.562, 9.274)
VIRADS	0.516	0.812	(0.433, 1.522)
Mean	0.001	0.874	(0.805, 0.949)
Median	0.920	0.999	(0.981, 1.017)
10 th percentile	0.726	0.998	(0.984, 1.011)
25 th percentile	0.001	1.081	(1.031, 1.133)
75 th percentile	0.007	1.057	(1.015, 1.100)
90 th percentile	0.625	1.003	(0.992, 1.014)

CI: confidence interval; VH: variant histology.

期及高分级,病灶呈浸润性生长且累及范围较广,因此病灶形态更常表现为宽基底附于膀胱壁。Li等^[21]研究也证实了在膀胱肿瘤中,分化出现与病灶分期、分级呈正相关。本研究发现伴有分化的膀胱癌患者增强扫描时更易出现不均匀强化(提示坏死、出血等),这可能是由于出现分化的肿瘤细胞侵袭性高,增殖速度快,代谢活跃,更易出现坏死,因此不均匀强化。在有分化出现的膀胱癌患者中,淋巴血管受侵也较常见。Rodler等^[22]使用CT图像评价有无出现分化膀胱癌患者的淋巴结转移情况,发现伴有其他病理亚型出现的膀胱癌患者更易出现淋巴结转移,预后差,与本研究结果一致。因此,MR

图像上膀胱肿瘤若表现为宽基底型/混合型且VI-RADS评分较高,增强扫描部分病灶不均匀强化且周围伴有可疑淋巴结转移,提示病理科医生应重点鉴别这部分患者病变组织是否伴有其他病理亚型的出现。

同时,本研究还采用基于全瘤体积的ADC直方图方法对预测膀胱癌患者是否出现其他病理亚型进行定量分析。ADC值可定量评估细胞间水分子运动情况,反映肿瘤组织结构及细胞数量,在膀胱癌中广泛应用于分级、分期及预后评估^[9,23-24]。基于病灶全容积的ADC直方图分析方法不仅可以提取多个反映肿瘤微观特征的定量参数从而全面、准确地对肿瘤进行分析评估,还可避免因局部ROI选择造成的主观性偏倚,使其测量结果可重复性提高^[12-14]。伴有分化的膀胱肿瘤侵袭性高,肿瘤细胞增殖活跃,使得肿瘤组织内细胞密度高,胞外间隙减小,肿瘤组织含水量下降。同时与单纯尿路上皮肿瘤相比,伴有其他病理亚型出现的肿瘤组织结构紊乱,可见细胞角化、腺性成分及其他异源成分混杂,使得水分子活动受限。上述原因导致有分化组各ADC直方图参数值小于无分化组($P < 0.05$)。先前研究报道不同百分位数在评估不同部位肿瘤的生物特征发挥的作用不同。本研究中ADC高百分位数(ADC_{75th}、ADC_{90th})的诊断效能高于低百分位数(ADC_{10th}、ADC_{25th})。近年来在膀胱癌相关研究中,Li等^[25]发现ADC高百分位数鉴别肌层及非肌层浸润性膀胱癌的诊断效能高于低百分位数,与本文研究结果一致。Zhang等^[26]预测肌层浸润性膀胱癌患者新辅助疗效时则发现ADC_{50th}诊断效能最佳。在其他癌种中,直肠癌^[27]、子宫内膜癌^[14]等相关研

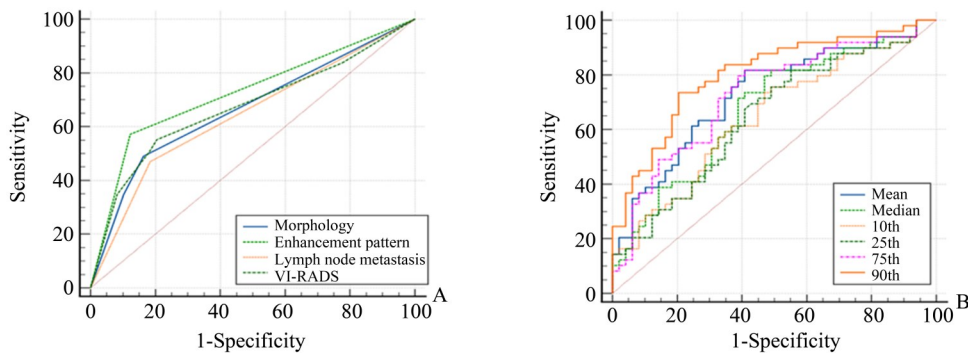


图4 影像学征象预测膀胱癌分化的ROC曲线(A)和ADC直方图参数预测膀胱癌分化的ROC曲线(B)

Fig. 4 ROC curve for the performance of imaging features in predicting VH(A) and ROC curve for the performance of ADC histogram features in predicting VH(B)

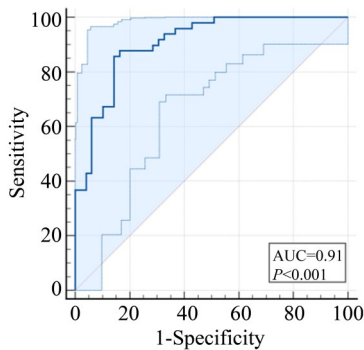


图5 影像学征象联合ADC直方图参数预测膀胱癌分化的ROC曲线

Fig. 5 ROC curve for the performance of imaging features combined with ADC histogram analysis in predicting VH

究结果与本文一致,但在部分恶性肿瘤,如肝癌^[28]、胃癌^[29]等,低百分位数诊断效能更好。这可能由于恶性肿瘤瘤内成分复杂,不同部位恶性肿瘤其组织结构有所差异,今后仍需大样本研究进一步探讨在膀胱癌中诊断效能最佳的ADC百分位数。

目前,在常规MRI形态学特征基础上增加功能成像研究成为诊断的重要方式之一。本研究进一步将有意义的MRI征象及ADC直方图参数纳入多因素logistic回归分析,发现病灶强化特点、ADC

mean、ADC_{25th}及ADC_{75th}为独立预测因子($P < 0.05$),将上述4个指标联合构建模型,预测概率AUC为0.91(95% CI: 0.83, 0.96),与单个指标相比差异均有统计学意义($P < 0.05$)。影像学征象与定量参数联合可以提高预测膀胱癌患者是否出现分化的准确性,对临床具有重要参考意义。

本研究首次采用多参数MRI预测膀胱癌患者是否出现其他病理亚型,目前仍存在一些局限性。首先,本研究采取倾向性匹配方法减少患者纳入时选择性偏倚,提高统计效能,但无法排除未纳入本研究的变量因素造成的信息偏倚。其次,本研究是单中心回顾性研究,伴有其他病理亚型分化的膀胱癌患者样本量较少。因此,本文仅将患者是否出现其他病理亚型分化作为分组条件,未进一步讨论不同程度病理亚型的表达及不同病理亚型之间差异。今后仍需前瞻性地在多中心、随机大样本人群中进一步研究证实,从而推广至临床。最后,本研究未能探讨扫描仪器、MRI系统参数的不同是否会对研究结果产生影响,今后仍需进一步研究探讨。

综上,多参数MRI定性征象联合定量指标可准确预测膀胱癌患者是否合并其他病理亚型的出现,有利于临床医生对膀胱癌患者全面评估,从而制定更加个体化的治疗方案,改善患者预后。

参考文献

- [1] Humphrey PA, Moch H, Cubilla AL, et al. The 2016 WHO classification of tumours of the urinary system and male genital organs—part B: prostate and bladder tumours [J]. *Eur Urol*, 2016, 70(1): 106–119.
- [2] Mitra AP, Bartsch CC, Bartsch G Jr, et al. Does presence of squamous and glandular differentiation in urothelial carcinoma of the bladder at cystectomy portend poor prognosis? an intensive case-control analysis [J]. *Urol Oncol*, 2014, 32(2): 117–127.
- [3] Nakagawa R, Iwamoto H, Makino T, et al. Squamous or glandular differentiation predicts poor prognosis in pT1 urothelial carcinoma [J]. *In Vivo*, 2022, 36(5): 2365–2370.
- [4] Vetterlein MW, SaMwankowicz, Seisen T, et al. Neoadjuvant chemotherapy prior to radical cystectomy for muscle-invasive bladder cancer with variant histology [J]. *Cancer*, 2017, 123(22): 4346–4355.
- [5] Wang M, Chen X, Tan P, et al. Acquired semi-squamization during chemotherapy suggests differentiation as a therapeutic strategy for bladder cancer [J]. *Cancer Cell*, 2022, 40(9): 1044–1059.
- [6] Willis D, Kamat AM. Nonurothelial bladder cancer and rare variant histologies [J]. *Hematol Oncol Clin North Am*, 2015, 29(2): 237–252.
- [7] Abd El-Latif A, Watts KE, Elson P, et al. The sensitivity of initial transurethral resection or biopsy of bladder tumor(s) for detecting bladder cancer variants on radical cystectomy [J]. *J Urol*, 2013, 189(4): 1263–1267.
- [8] Hong SB, Lee NK, Kim S, et al. Vesical imaging-reporting and data system for multiparametric MRI to predict the presence of muscle invasion for bladder cancer [J]. *J Magn Reson Imaging*, 2020, 52(4): 1249–1256.
- [9] Wang HJ, Cai Q, Huang YP, et al. Amide proton transfer-weighted MRI in predicting histologic grade of bladder cancer [J]. *Radiology*, 2022;305(1): 127–134.
- [10] Xu X, Wang H, Du P, et al. A predictive nomogram for individualized recurrence stratification of bladder cancer using

- multiparametric MRI and clinical risk factors[J]. *J Magn Reson Imaging*, 2019, 50(6): 1893-1904.
- [11] De Perrot T, Sadjo Zoua C, Glessgen CG, et al. Diffusion-weighted MRI in the genitourinary system [J]. *J Clin Med*, 2022;11(7):1921.
- [12] Li Q, Xiao Q, Yang M, et al. Histogram analysis of quantitative parameters from synthetic MRI: correlations with prognostic factors and molecular subtypes in invasive ductal breast cancer[J]. *Eur J Radiol*, 2021, 139: 109697.
- [13] Li X, Hu Y, Xie Y, et al. Whole-tumor histogram analysis of diffusion-weighted imaging and dynamic contrast-enhanced MRI for soft tissue sarcoma: correlation with HIF-1 α expression[J]. *Eur Radiol*, 2023, 33(6): 3961-3973.
- [14] Meyer HJ, Hamerla G, Höhn AK, et al. Whole Lesion Histogram analysis derived from morphological MRI sequences might be able to predict EGFR- and Her2-Expression in cervical cancer[J]. *Acad Radiol*, 2019, 26(8): e208-e215.
- [15] Tsili AC, Astrakas LG, Goussia AC, et al. Volumetric apparent diffusion coefficient histogram analysis of the testes in non-obstructive azoospermia: a noninvasive fingerprint of impaired spermatogenesis? [J]. *Eur Radiol*, 2022, 32(11): 7522-7531.
- [16] Netto GJ, Amin MB, Berney DM, et al. The 2022 world health organization classification of tumors of the urinary system and male genital organs-part B: prostate and urinary tract tumors[J]. *Eur Urol*, 2022, 82(5): 469-482.
- [17] Moschini M, D'andrea D, Korn S, et al. Characteristics and clinical significance of histological variants of bladder cancer [J]. *Nat Rev Urol*, 2017, 14(11): 651-668.
- [18] Hajiran A, Azizi M, Aydin AM, et al. Pathological and survival outcomes associated with variant histology bladder cancers managed by cystectomy with or without neoadjuvant chemotherapy[J]. *J Urol*, 2021, 205(1): 100-108.
- [19] Mehrmouh V, Brennan L, Ismail A, et al. Radical cystectomy for bladder urothelial carcinoma with aggressive variant histology[J]. *Arch Ital Urol Androl*, 2022, 94(3): 291-294.
- [20] Zamboni S, Afferi L, Soria F, et al. Adjuvant chemotherapy is ineffective in patients with bladder cancer and variant histology treated with radical cystectomy with curative intent [J]. *World J Urol*, 2021, 39(6): 1947-1953.
- [21] 李曾, 毛顿, 廖洪, 等. 膀胱浸润性尿路上皮癌部分亚型的临床病理特征分析[J]. *肿瘤预防与治疗*, 2021, 34(6): 555-561.
- Li Z, Mao D, Liao H, et al. Clinicopathological analysis of some subtypes of invasive urothelial carcinoma of the bladder [J]. *J cancer Contr and Treat*, 2021, 34(6): 555-561.
- [22] Rodler S, Solyanik O, Ingenerf M, et al. Accuracy and prognostic value of radiological lymph node features in variant histologies of bladder cancer[J]. *World J Urol*, 2022, 40(7): 1707-1714.
- [23] Zhang W, Zhang Z, Xiao W, et al. Multiple directional DWI combined with T2WI in predicting muscle layer and Ki-67 correlation in bladder cancer in 3.0-T MRI[J]. *Cancer Med*, 2023;12(9):10462-10472.
- [24] Xu S, Yao Q, Liu G, et al. Combining DWI radiomics features with transurethral resection promotes the differentiation between muscle-invasive bladder cancer and non-muscle-invasive bladder cancer[J]. *Eur Radiol*, 2020, 30(3): 1804-1812.
- [25] Li S, Liang P, Wang Y, et al. Combining volumetric apparent diffusion coefficient histogram analysis with vesical imaging reporting and data system to predict the muscle invasion of bladder cancer [J]. *Abdom Radiol (NY)*, 2021, 46(9): 4301-4310.
- [26] Zhang X, Wang Y, Zhang J, et al. Muscle-invasive bladder cancer: pretreatment prediction of response to neoadjuvant chemotherapy with diffusion-weighted MR imaging [J]. *Abdom Radiol (NY)*, 2022, 47(6): 2148-2157.
- [27] 董立杰, 张林, 杲霄源, 等. 全病灶ADC直方图分析在直肠癌组织学分级的临床应用研究[J]. *磁共振成像*, 2022, 13(7):48-54.
- Dong LJ, Zhang L, Gao XY, et al. Clinical application of whole-volume apparent diffusion coefficient histogram parameters of histological grading rectal adenocarcinoma[J]. *Chin J Magn Reson Imaging*, 2022, 13(7):48-54.
- [28] Xu YS, Liu HF, Xi DL, et al. Whole-lesion histogram analysis metrics of the apparent diffusion coefficient: a correlation study with histological grade of hepatocellular carcinoma [J]. *Abdom Radiol (NY)*, 2019, 44(9): 3089-3098.
- [29] Zhang Y, Chen J, Liu S, et al. Assessment of histological differentiation in gastric cancers using whole-volume histogram analysis of apparent diffusion coefficient maps[J]. *J Magn Reson Imaging*, 2017, 45(2): 440-449.

(编辑 孙慧兰)